

Measuring the SUSY Mass Scale at the LHC

D.R. Tovey *

*Department of Physics and Astronomy, University of Sheffield,
Hounsfield Road, Sheffield S3 7RH, UK.*

Abstract

An effective mass scale $M_{\text{susy}}^{\text{eff}}$ for supersymmetric particles is defined and techniques for its measurement at the LHC discussed. Monte Carlo results show that, for jets + E_T^{miss} events, a variable constructed from the scalar sum of the transverse momenta of all reconstructed jets together with E_T^{miss} provides in most cases the most accurate model independent measurement of $M_{\text{susy}}^{\text{eff}}$ (intrinsic precision ~ 2.1 % for mSUGRA models). The overall precision with which $M_{\text{susy}}^{\text{eff}}$ could be measured after given periods of LHC running and for given classes of SUSY models is calculated. The technique is extended to measurements of the total SUSY particle production cross section σ_{susy} .

PACS: 12.60.Jv; 14.80.Ly; 04.65.+e

Keywords: LHC; supersymmetry; model; measurement

* e-mail: d.r.tovey@sheffield.ac.uk

1 Introduction

One of the principal motivations for construction of the Large Hadron Collider is the search for low energy supersymmetry (SUSY) [1]. In a large class of models the interactions of SUSY particles conserve R-parity, causing the Lightest Supersymmetric Particle (LSP) to be neutral and stable. R-Parity conserving SUSY events at hadron colliders are predicted to consist of cascade decays of heavy, strongly interacting SUSY particles into lighter Standard Model (SM) particles and two LSPs. This results in the classic discovery signature of an excess of events containing jets, leptons and large quantities of event missing transverse energy E_T^{miss} [2].

Should R-Parity conserving SUSY particles be discovered at the LHC the next task would be to measure their properties. Importantly, such measurements must be independent of the SUSY model and its parameters, which are *a priori* unknown. This process is complicated by lack of knowledge of the momenta of the two escaping LSPs in each event, preventing direct reconstruction of SUSY particle masses. Consequently other techniques are required which can measure masses or combinations of masses indirectly. With sufficient integrated luminosity it should be possible to look for edges in the invariant mass spectra of various combinations of jets and leptons in SUSY events [2, 3], but initially the most effective technique is likely to be the use of distributions of event transverse momentum p_T and missing transverse energy [3]. In this letter, the latter technique will be investigated in detail and extended to SUSY models beyond the minimal Supergravity (mSUGRA) models considered previously [3].

2 Measurement Technique

Consider a heavy SUSY particle (mass m_1) produced in a hadron-hadron collision. Assume further that this particle is boosted along the beam-axis by the longitudinal momentum imbalance of the event. If this particle undergoes a cascade decay to a lighter SUSY particle (mass m_2) and a Standard Model particle (assumed massless), then the transverse momentum p_T of the SM particle in the lab frame is related to m_1 and m_2 :

$$p_T \propto \frac{1}{2} \left(m_1 - \frac{m_2^2}{m_1} \right). \quad (1)$$

Variables based on the p_T of SM particles in SUSY events are therefore sensitive to SUSY particle masses, modulo smearing effects arising from the true η distribution of those particles.

Events in the jets + E_T^{miss} + 0 leptons channel were used for this study. The lepton veto requirement was imposed to reduce possible systematics in the measurement arising from SM neutrino production. Defining $p_{T(i)}$ as the transverse momentum of jet i (arranged in descending order of p_T), the following four measurement variables M_{est} were studied:

- (1) $M_{\text{est}} = |p_{T(1)}| + |p_{T(2)}| + |p_{T(3)}| + |p_{T(4)}| + E_T^{\text{miss}},$
- (2) $M_{\text{est}} = |p_{T(1)}| + |p_{T(2)}| + |p_{T(3)}| + |p_{T(4)}|,$
- (3) $M_{\text{est}} = \sum_i |p_{T(i)}| + E_T^{\text{miss}},$
- (4) $M_{\text{est}} = \sum_i |p_{T(i)}|.$

The first variable is identical to the “effective mass” variable (M_{eff}) defined in Ref. [3]. The scalar sum of the transverse momenta of only the four hardest jets was used due to the predominantly four-jet nature of many SUSY events [4], while the addition of the event E_T^{miss} accounts for the p_T carried away by the LSPs.

Combining all jets in each detector hemisphere j into one pseudo-particle of transverse momentum $p_{T(j)}$ and invariant mass m_j , a fifth variable was also defined:

$$(5) \quad M_{\text{est}} = \frac{1}{2} \sum_{j=1}^2 \sqrt{m_j^2 + 4p_{T(j)}^2} + 2\sqrt{(m_x^2 + 2p_{T(j)}^2) \cdot (m_j^2 + 2p_{T(j)}^2)},$$

where $m_x = 100 \text{ GeV}/c^2$. This variable approximates the mean of the reconstructed masses of the two initial SUSY particles, assuming that each moves close to the beam axis and decays into an LSP with mass of order m_x .

3 Definition of Mass Scale

Due to the large number of different SUSY particles which can be produced in any given event masses measured with these variables will not correspond to those of any one particular SUSY state. Nevertheless in many models the strongly interacting SUSY particles are considerably heavier than states further down the decay chain. Hence it is the decays of these particles which will contribute most to the sum of $|p_T|$. For this reason we shall choose to define a SUSY “mass scale” M_{susy} as the weighted mean of the masses of the initial SUSY particles, with the weighting provided by the production cross section of each state:

$$M_{\text{susy}} = \frac{\sum_i \sigma_i m_i}{\sum_i \sigma_i}. \quad (2)$$

This definition differs from that used in Ref. [3] but in the limit where squarks or gluinos of a single mass dominate the production cross section it gives the same result.

The above approximation breaks down for models where the lighter SUSY particles are of similar mass to the strongly interacting states. We shall attempt to compensate for this when using variables (1) - (4) by defining an effective SUSY mass scale $M_{\text{susy}}^{\text{eff}}$ in analogy with Eqn. (1):

$$M_{\text{susy}}^{\text{eff}} = \left(M_{\text{susy}} - \frac{M_\chi^2}{M_{\text{susy}}} \right), \quad (3)$$

where M_χ is the mass of the LSP. For variable (5) the equivalent expression is somewhat different:

$$M_{\text{susy}}^{\text{eff}} = \sqrt{M_{\text{susy}}^2 - M_\chi^2}. \quad (4)$$

With these definitions of the effective SUSY mass scale comparison of experimental results with the predictions of a given SUSY model requires knowledge of the model dependent particle mass spectrum and production cross sections.

4 Simulation and Event Selection

Events were generated using PYTHIA 6.115 [5] (SM background, mSUGRA and MSSM signal) and ISAJET 7.44 [6] (GMSB signal). Hadronized events were passed through a simple simulation of a generic LHC detector. The calorimeter was assumed to have granularity $\Delta\eta \times \Delta\phi = 0.1 \times 0.1$ over the range $|\eta| < 5$, and energy resolutions $10\%/\sqrt{E} \oplus 1\%$ (ECAL), $50\%/\sqrt{E} \oplus 3\%$ (HCAL) and $100\%/\sqrt{E} \oplus 7\%$ (FCAL; $|\eta| > 3$). Jets were found with the GETJET [6] fixed cone algorithm with cone radius $\Delta R = 0.5$ and $E_T^{cut} = 50$ GeV.

Events in the jets + E_T^{miss} channel were selected with the following criteria:

- ≥ 4 jets with $p_T \geq 50$ GeV
- ≥ 2 jets with $p_T \geq 100$ GeV
- $E_T^{\text{miss}} \geq \max(100 \text{ GeV}, 0.25 \sum_i p_{T(i)})$
- Transverse Sphericity $S_T \geq 0.2$
- $\Delta\phi_{(\mathbf{p}_{T(1)}, \mathbf{p}_{T(2)})} \leq 170^\circ$
- $\Delta\phi_{(\mathbf{p}_{T(1)} + \mathbf{p}_{T(2)}, \mathbf{E}_T^{\text{miss}})} \leq 90^\circ$
- No muons or isolated electrons with $p_T > 10$ GeV in $|\eta| < 2.5$.

Standard Model background events were generated for the following processes: $t\bar{t}$ (5×10^4 events), $W + \text{jet}$ (5×10^4 events), $Z + \text{jet}$ (5×10^4 events) and QCD $2 \rightarrow 2$ processes [5] (2.5×10^6 events). The distributions of the M_{est} variables for these events were then compared with those for SUSY signal events generated from the mSUGRA (minimal Supergravity [1]), MSSM (Minimal Supersymmetric Standard Model¹[1]) and GMSB (Gauge Mediated SUSY Breaking [8]) models. In each case 100 points were randomly chosen from within the parameter space of the model, and 1×10^4 events (a factor 10 greater than in Ref. [3]) generated for each point.

For mSUGRA models the region of parameter space sampled was identical to that used in Ref. [3]: $100 \text{ GeV} < m_0 < 500 \text{ GeV}$, $100 \text{ GeV} < m_{1/2} < 500 \text{ GeV}$, $-500 \text{ GeV} < A_0 < 500 \text{ GeV}$, $1.8 < \tan(\beta) < 12.0$ and $\text{sign}(\mu) = \pm 1$. For MSSM models the choice of points was complicated by the requirement that models be physically realistic (positive particle masses etc.) and be suitable for this study (neutralino LSP). The masses of the strongly interacting SUSY particles and sleptons were constrained to lie in the range from $250 \text{ GeV}/c^2$ to $2000 \text{ GeV}/c^2$ while the mass parameters of the partners of the electroweak gauge bosons were constrained to lie in the range from $50 \text{ GeV}/c^2$ to the mass of the lightest strongly interacting SUSY particle or slepton. $\tan(\beta)$ was constrained to lie in the range $1.4 < \tan(\beta) < 100.0$. Finally, given that the lightest SUSY particles in models with low $M_{\text{susy}}^{\text{eff}}$ have a high probability of discovery before LHC comes on line, only those models with $M_{\text{susy}}^{\text{eff}} > 250 \text{ GeV}/c^2$ were used.

In mSUGRA and MSSM models the LSP is generally the lightest neutralino χ_1^0 , but in GMSB models this role is taken by the gravitino. If the Next-to-Lightest Supersymmetric Particle (NLSP) is neutral and sufficiently long-lived to escape from the detector then the

¹A constrained version of the MSSM with 15 free parameters (no additional D-terms, 3rd generation trilinear couplings derived from masses) implemented in SPYTHIA [7]

phenomenology is similar to that for mSUGRA or MSSM models [9]. If the NLSP is short-lived however then it decays to a gravitino and the phenomenology is different. To test whether the M_{est} variables defined above are also sensitive to the effective mass scales of these latter models points were chosen from within the range of GMSB parameter space defined by: $10 \text{ TeV} < \Lambda_m < 100 \text{ TeV}$, $100 \text{ TeV} < M_m < 1000 \text{ TeV}/c^2$, $1 < N_5 < 5$, $1.8 < \tan(\beta) < 12.0$ and $\text{sign}(\mu) = \pm 1$. The value of C_{grav} , the ratio of the gravitino mass to that expected for only one SUSY breaking scale [6], was set to unity in all cases to ensure rapid decays to the gravitino LSP. Again only those models with $M_{\text{susy}}^{\text{eff}} > 250 \text{ GeV}/c^2$ were used.

In the mSUGRA and MSSM models a statistically significant excess of signal events (S) above background (B) ($\sqrt{S+B} - \sqrt{B} \geq 5.0$ [10]) was found for the majority of points after the delivery of only 10 fb^{-1} of integrated luminosity (1 year of low luminosity operation). In GMSB models the data indicate that greater event statistics corresponding to at least 100 fb^{-1} (1 year of high luminosity running) would be required for discovery with these particular cuts. It should be noted however that the use of this channel and these cuts has been optimised for mSUGRA points. In GMSB models with prompt decays to gravitino LSPs photon production (bino NLSP) or lepton production (slepton NLSP) is common [11] and consequently many events were rejected by the lepton veto and jet multiplicity requirements. In dedicated GMSB studies these requirements should therefore be loosened in order to increase signal acceptance. In this case measurement variables taking account of lepton and/or photon p_T should also be used to reduce systematic measurement errors [11].

5 Mass Scale Measurement

The M_{est} distributions of SUSY signal events in the models considered here are roughly gaussian in shape (see Figs. (1) - (5) of Ref. [3]), in sharp contrast to the SM background which falls rapidly with M_{est} . Fitting gaussian curves to the signal distributions then provides estimates of their means which can be compared with the effective mass scales $M_{\text{susy}}^{\text{eff}}$ of the corresponding SUSY models. The degree of correlation between the two variables gives a measure of the intrinsic (systematic) precision provided by the M_{est} variable when measuring $M_{\text{susy}}^{\text{eff}}$.

A typical scatter plot of $M_{\text{susy}}^{\text{eff}}$ against M_{est} (here variable (3)) for mSUGRA models is shown in Fig. 1(a). The correlation between the variables is clearly very good. To quantify the degree of correlation a linear regression was performed on the data and the points projected onto an axis perpendicular to the fitted trendline. The distribution of the data along this line for mSUGRA models is shown in Fig. 2(a).

A scatter plot of $M_{\text{susy}}^{\text{eff}}$ against M_{est} variable (3) for MSSM models is shown in Fig. 1(b). In Figs. 2(b) and (c) are plotted correlation histograms derived from this figure using the projection axis defined by the mSUGRA data. Fig. 2(b) shows the histogram obtained assuming $M_{\text{susy}}^{\text{eff}} = M_{\text{susy}}$, while Fig. 2(c) shows the equivalent histogram using the definition of $M_{\text{susy}}^{\text{eff}}$ in Eqn. (3). The smaller scatter in this latter case indicates an improved measurement precision. An improvement is also obtained for mSUGRA models. Here however it is smaller since M_χ is usually much less than the masses of the strongly interacting SUSY particles [12]. In GMSB models (Fig. 1(c) and Fig. 2(d)) M_χ is negligible and so the two definitions of $M_{\text{susy}}^{\text{eff}}$ are always identical.

The correlation histograms were next fitted with gaussian functions. The fitted values

widths σ were used to calculate the intrinsic measurement precision by subtracting in quadrature the width expected from finite event statistics (assumed to be given by the rms of the errors on the fitted means of the M_{est} distributions). Due to uncertainties in the expected statistical scatter this correction could give unduly optimistic estimates of the measurement precision if it were large. In all cases however the corrections were found to be small ($\lesssim 33\%$) and the effects of such uncertainties neglected.

Intrinsic measurement precisions for $M_{\text{susy}}^{\text{eff}}$ calculated using the above technique for mSUGRA, MSSM and GMSB models and the five M_{est} variables listed in Sec. 2 are presented in Table 1. Variable (3) ($M_{\text{est}} = \sum_i |p_{T(i)}| + E_T^{\text{miss}}$) provides the greatest precision for mSUGRA and MSSM models, with the higher precision being for mSUGRA models (2.1 %). The poorer precision for MSSM models (12.8 %) is due to their greater number of free parameters and hence the smaller correlation between the particle masses. In the GMSB models variable (4) ($M_{\text{est}} = \sum_i |p_{T(i)}|$) provides the greatest measurement precision (6.1 %), however variable (3) is reasonably accurate (9.0 %). This indicates that effective mass scale measurements are also effective for models with gravitino LSPs.

It should be noted that for any given M_{est} variable the fitted means of the projected histograms (Table 1) for mSUGRA, MSSM and GMSB models are consistent to within the fitted widths. For this reason it can be said that the variables provide *model independent* measurements of the effective SUSY mass scale $M_{\text{susy}}^{\text{eff}}$. The expected measurement precision is SUSY model dependent (due to larger widths for MSSM histograms than for mSUGRA and GMSB histograms) but this is less troublesome when comparing measurements with theory because in this case a particular SUSY model must be assumed.

With the intrinsic precision from Table 1 for M_{est} variable (3) it is possible to estimate the overall (systematic + statistical) precision for measuring effective SUSY mass scales in mSUGRA, MSSM and GMSB models as a function of the mass scale and integrated luminosity. Distributions of M_{est} for signal + background events were first constructed assuming integrated luminosities of 10 fb^{-1} (1 year low luminosity), 100 fb^{-1} (1 year high lumi.) and 1000 fb^{-1} (10 years high lumi.). The mean background distribution was then subtracted from each with an assumed 50% systematic error ². The resulting distributions were again fitted with gaussian functions and the errors on the fitted means added in quadrature to the intrinsic precision calculated above and an estimated 1% systematic error from uncertainties in the measurement of the jet energy scale.

The results are plotted in Fig. 3 for mSUGRA, MSSM and GMSB models. In the last case results for 100 fb^{-1} and 1000 fb^{-1} only are presented due to the poor statistical significance of GMSB models in the jets + E_T^{miss} channel at low integrated luminosity. Precisions $\lesssim 15\%$ (40%) should be achievable in mSUGRA (MSSM) models after only one year of low luminosity running, improving to $\lesssim 7\%$ (20%) after one year of high luminosity running. Due to the poor statistics obtainable from GMSB models, particularly for high $M_{\text{susy}}^{\text{eff}}$ values, measurement precisions $\lesssim 50\%$ are likely to be obtainable with these cuts only after the delivery of 1000 fb^{-1} of integrated luminosity and for $M_{\text{susy}}^{\text{eff}} \lesssim 1000 \text{ GeV}/c^2$.

²It is unlikely that the distribution of background events (especially QCD) will be known with any certainty from theory. Instead the distribution of low E_T^{miss} events will likely be measured and the results extrapolated into the high E_T^{miss} region [13, 14]. 50% is a conservative estimate of the systematic uncertainty associated with this extrapolation.

6 Cross Section Measurement

The above technique can also be used to measure the total SUSY production cross section σ_{susy} , although in this case it is the fitted normalisation of the signal M_{est} distribution which is of interest. The correlation between this normalisation and σ_{susy} for M_{est} variable (3) is shown in Fig. 4. The correlation is reasonably good with the data best fitted by a power-law. For these measurements the errors are non-gaussian (due to the power-law relation between the normalisation and σ_{susy}) and in reality it is the logarithm of the measured cross sections which is approximately gaussian distributed. For this reason the intrinsic measurement precisions for $\ln(\sigma_{\text{susy}})$ are listed in Table 2. The overall (non-gaussian) precisions for σ_{susy} (i.e. $d\sigma_{\text{susy}}/\sigma_{\text{susy}} = d(\ln(\sigma_{\text{susy}}))$) are plotted in Fig. 5 in the same format as Fig. 3. For mSUGRA models the overall σ_{susy} measurement precision obtainable for 1000 fb^{-1} is $\lesssim 15 \%$, while for MSSM models it is $\lesssim 50 \%$.

Measurements of σ_{susy} carried out in this way are inherently sensitive to the type of SUSY model, in contrast to the measurements of $M_{\text{susy}}^{\text{eff}}$. This is because in some models (e.g. GMSB) the SUSY particle decay characteristics can be such that the probability for signal events to pass the selection cuts is reduced significantly relative to that for mSUGRA models. The analysis presented here is intended to be model independent and so projects data onto a single axis perpendicular to the trendline of the mSUGRA models. Consequently in the GMSB case, where the trend is very different from that for mSUGRA, the presented measurement precision is poor ($\gtrsim 300 \%$). If it were known that GMSB models were correct then an axis perpendicular to the GMSB trendline could be used to obtain much greater measurement precision ($\ln(\sigma_{\text{susy}})$ precision $< 2.5 \%$). This highlights the fact that in reality measurements of σ_{susy} , unlike measurements of $M_{\text{susy}}^{\text{eff}}$, are dependent on the assumed SUSY model.

7 Conclusions

Model independent techniques for measuring the effective mass scale of SUSY particles at the LHC have been investigated. Overall measurement precisions better than 15 % (40 %) should be possible for mSUGRA (MSSM) models after only one year of running at low luminosity. Measurements should also be possible for models with rapid decays to gravitino LSPs, although with the requirement of either significantly increased statistics or measurement variables using photon or lepton p_T . The total SUSY production cross section should be measureable in a similar way ultimately to $\sim 15 \%$ (50 %) in mSUGRA (MSSM) models, although not in a completely model independent manner.

Acknowledgments

The author wishes to thank Frank Paige and Craig Buttar for their careful reading of this manuscript and many helpful comments and suggestions. He also wishes to acknowledge PPARC for support under the Post-Doctoral Fellowship program.

References

- [1] H.P. Nilles, *Phys. Rep.* **111** (1984) 1; H.E. Haber, G.L. Kane, *Phys. Rep.* **117** (1985) 75.
- [2] H. Baer, C.-H. Chen, F. Paige, X. Tata, *Phys. Rev.* **D52** (1995) 2746; *Phys. Rev.* **D53** (1996) 6241.
- [3] I. Hinchliffe, F.E. Paige, M.D. Shapiro, J. Söderqvist, W. Yao, *Phys. Rev.* **D55** (1997) 5520 9.
- [4] F.E. Paige, *hep-ph/9801254*.
- [5] T. Sjöstrand, *Comput. Phys. Commun.* **82** (1994) 74.
- [6] F. Paige, S. Protopopescu, in *Supercollider Physics*, ed. D. Soper (World Scientific, 1986); H. Baer, F. Paige, S. Protopopescu, X. Tata, in *Proc. Workshop on Physics at Current Accelerators and Supercolliders*, ed. J. Hewett, A. White, D. Zeppenfeld (Argonne National Laboratory, 1993).
- [7] S. Mrenna, *Comput. Phys. Commun.* **101** (1997) 232.
- [8] M. Dine, W. Fischler, M. Srednicki, *Nucl. Phys.* **B189** (1981) 575.
- [9] I. Hinchliffe, F.E. Paige, *Phys. Rev.* **D60** (1999) 9 095002/1.
- [10] S.I. Bityukov, N.V. Krasnikov, *hep-ph/9908492*.
- [11] F.E. Paige, *Private Communication*.
- [12] M. Drees, S.P. Martin, in *Electroweak Symmetry Breaking and Beyond the Standard Model*, ed. T. Barklow, S. Dawson, H. Haber, S. Siegrist (World Scientific, 1995) 146.
- [13] F. Abe *et al.*, *Phys. Rev. Lett.* **76** (1996) 2006.
- [14] B. Abbott *et al.*, *Phys. Rev. Lett.* **83** (1999) 4937 24.

Tables

Table 1: Estimates of the intrinsic $M_{\text{susy}}^{\text{eff}}$ measurement precision for mSUGRA, MSSM and GMSB models for the five M_{est} variables discussed in the text. The third and fourth columns show the fitted mean and width of the projected $M_{\text{susy}}^{\text{eff}}$ - M_{est} correlation histogram for each model and variable, and the fifth column their ratio. The sixth column shows the expected fractional width estimated from the rms error on the fitted means of the signal distributions. The seventh column contains the intrinsic measurement precision estimated by subtracting in quadrature column six from column five.

Table 2: Estimates of the intrinsic $\ln(\sigma_{\text{susy}})$ measurement precision for mSUGRA, MSSM and GMSB models for M_{est} variable (3) (defined in the text). The third and fourth columns show the fitted mean and width of the projected $\ln(\sigma_{\text{susy}})$ - normalisation correlation histogram for each model and variable, and the fifth column their ratio. The sixth column shows the expected fractional width estimated from the rms error on the fitted normalisations of the signal distributions. The seventh column contains the intrinsic measurement precision estimated by subtracting in quadrature column six from column five.

Figures

Figure 1: The effective SUSY mass scale $M_{\text{susy}}^{\text{eff}}$ plotted against M_{est} for variable (3) (defined in the text) for 100 random mSUGRA (Fig. 1(a)), MSSM (Fig. 1(b)) and GMSB (Fig. 1(c)) models. Note the differing scale in Fig. 1(c) due to the larger spread in M_{est} values generated for GMSB models. In Fig. 1(c) those GMSB models where the gaussian fit to the signal M_{est} distribution failed due to insufficient acceptance are omitted.

Figure 2: Projections of the points in Fig. 1 onto an axis transverse to the fitted trend-line of mSUGRA data (Fig. 1(a)) for M_{est} variable (3). Fig. 2(a) shows the distribution for mSUGRA points, Fig. 2(b) the distribution for MSSM points with $M_{\text{susy}}^{\text{eff}} = M_{\text{susy}}$, Fig. 2(c) the distribution for MSSM points with $M_{\text{susy}}^{\text{eff}}$ given by Eqn. (3) and Fig. 2(d) the distribution for GMSB points. Bin widths are equal in Fig. 2(b) and Fig. 2(c) to aid comparison. Bin widths differ between other plots.

Figure 3: Overall precision for measurement of $M_{\text{susy}}^{\text{eff}}$ after delivery of integrated luminosities of 10 fb^{-1} (stars), 100 fb^{-1} (open circles) and 1000 fb^{-1} (filled circles) for M_{est} variable (3). Precisions for mSUGRA points are plotted in Fig. 3(a), MSSM points in Fig. 3(b) and GMSB points in Fig. 3(c). No data are shown for GMSB points for 10 fb^{-1} integrated luminosity due to the poor statistical significance of signal events in this scenario. Note the differing scale in Fig. 3(c) due to the larger spread in M_{est} values generated for GMSB models.

Figure 4: The total SUSY particle production cross section σ_{susy} plotted against the fitted normalisation of the signal distribution for variable (3) (defined in the text) for 100 random mSUGRA (Fig. 4(a)), MSSM (Fig. 4(b)) and GMSB (Fig. 4(c)) models. In Fig. 4(c) those GMSB models where the gaussian fit to the signal M_{est} distribution failed due to insufficient acceptance are omitted.

Figure 5: Overall (non-gaussian) precision for measurement of σ_{susy} after delivery of integrated luminosities of 10 fb^{-1} (stars), 100 fb^{-1} (open circles) and 1000 fb^{-1} (filled circles) for M_{est} variable (3). Precisions for mSUGRA points are plotted in Fig. 5(a), MSSM points in Fig. 5(b) and GMSB points in Fig. 5(c). No data are shown for GMSB points for 10 fb^{-1} integrated luminosity due to the poor statistical significance of signal events in this scenario. Note the differing scale in Fig. 5(c) due to the larger spread in M_{est} values generated for GMSB models.

Model	Variable	\bar{x}	σ	σ/\bar{x}	rms error (\bar{x})	Precision (%)
mSUGRA	1	1.585	0.049	0.031	0.011	2.9
	2	0.991	0.039	0.039	0.010	3.8
	3	1.700	0.043	0.026	0.015	2.1
	4	1.089	0.030	0.028	0.011	2.5
	5	1.168	0.029	0.025	0.013	2.1
MSSM	1	1.657	0.386	0.233	0.031	23.1
	2	0.998	0.214	0.215	0.042	21.1
	3	1.722	0.227	0.132	0.031	12.8
	4	1.092	0.143	0.131	0.029	12.8
	5	1.156	0.176	0.152	0.034	14.8
GMSB	1	1.660	0.149	0.090	0.037	8.1
	2	1.095	0.085	0.077	0.040	6.6
	3	1.832	0.176	0.096	0.034	9.0
	4	1.235	0.091	0.074	0.041	6.1
	5	1.273	0.109	0.086	0.034	7.9

Table 1:

Model	Variable	\bar{x}	σ	σ/\bar{x}	rms error (\bar{x})	Precision (%)
mSUGRA	3	0.855	0.008	0.009	0.003	0.8
MSSM	3	0.848	0.023	0.027	0.004	2.7
GMSB	3	0.742	0.141	0.190	0.006	19.0

Table 2:

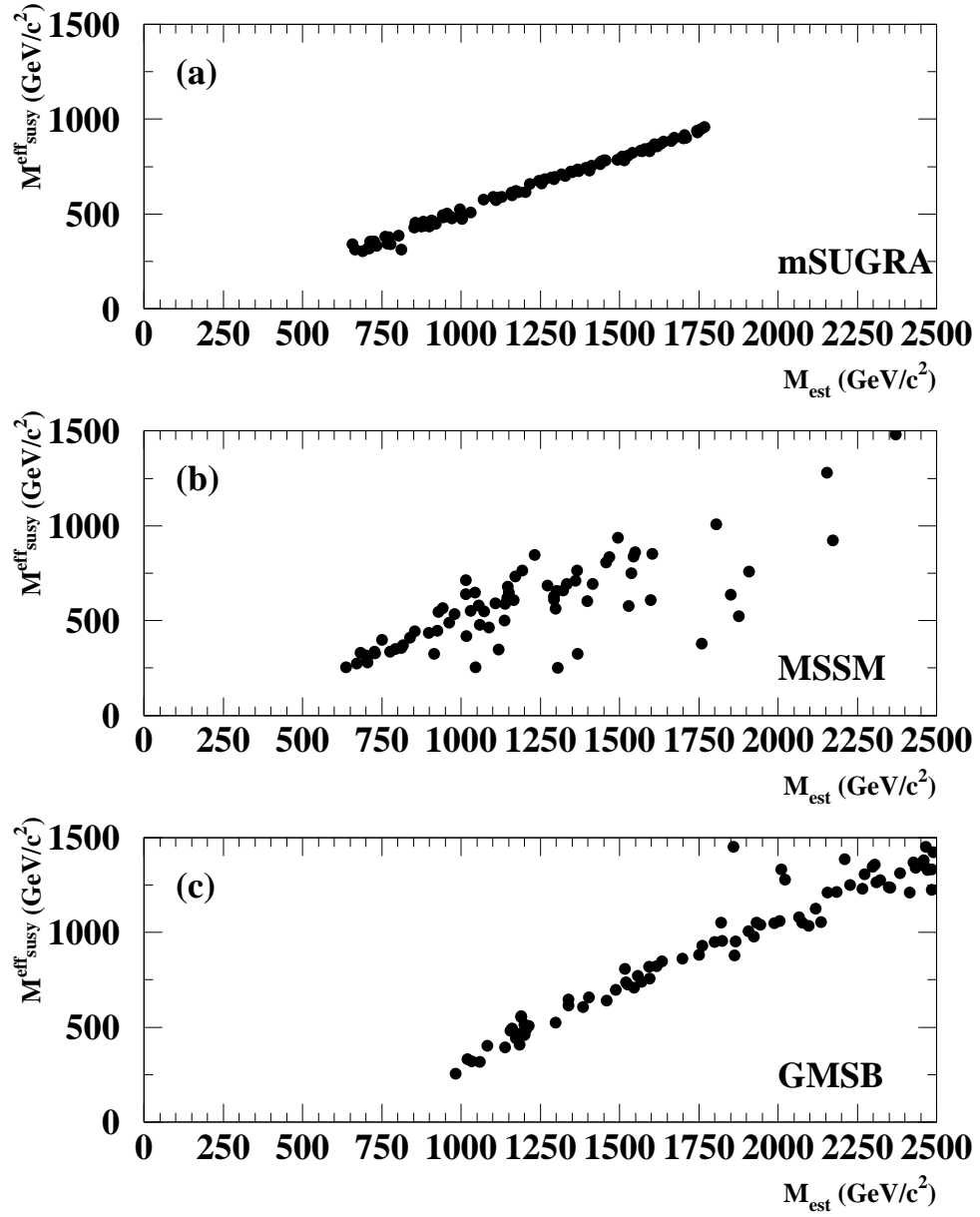


Figure 1:

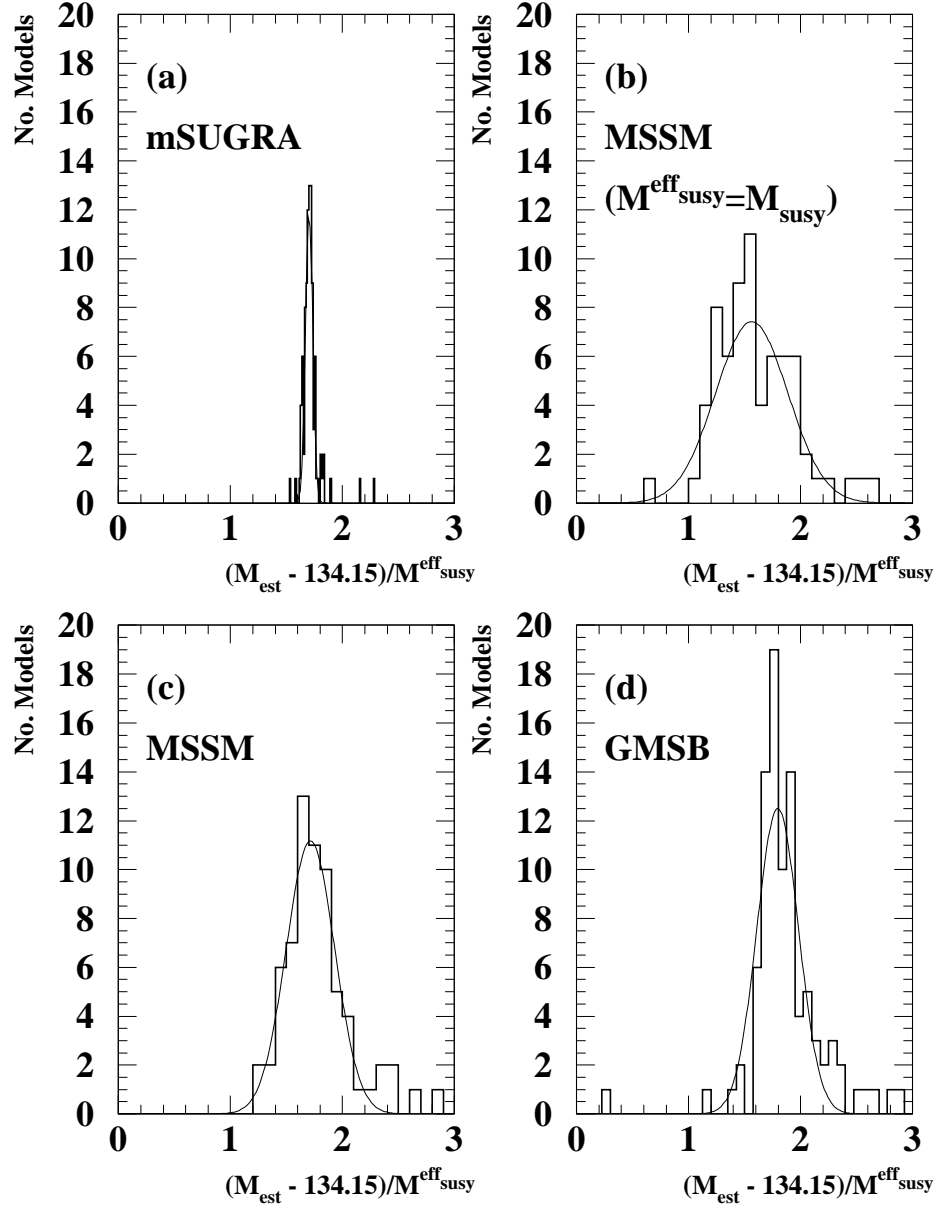


Figure 2:

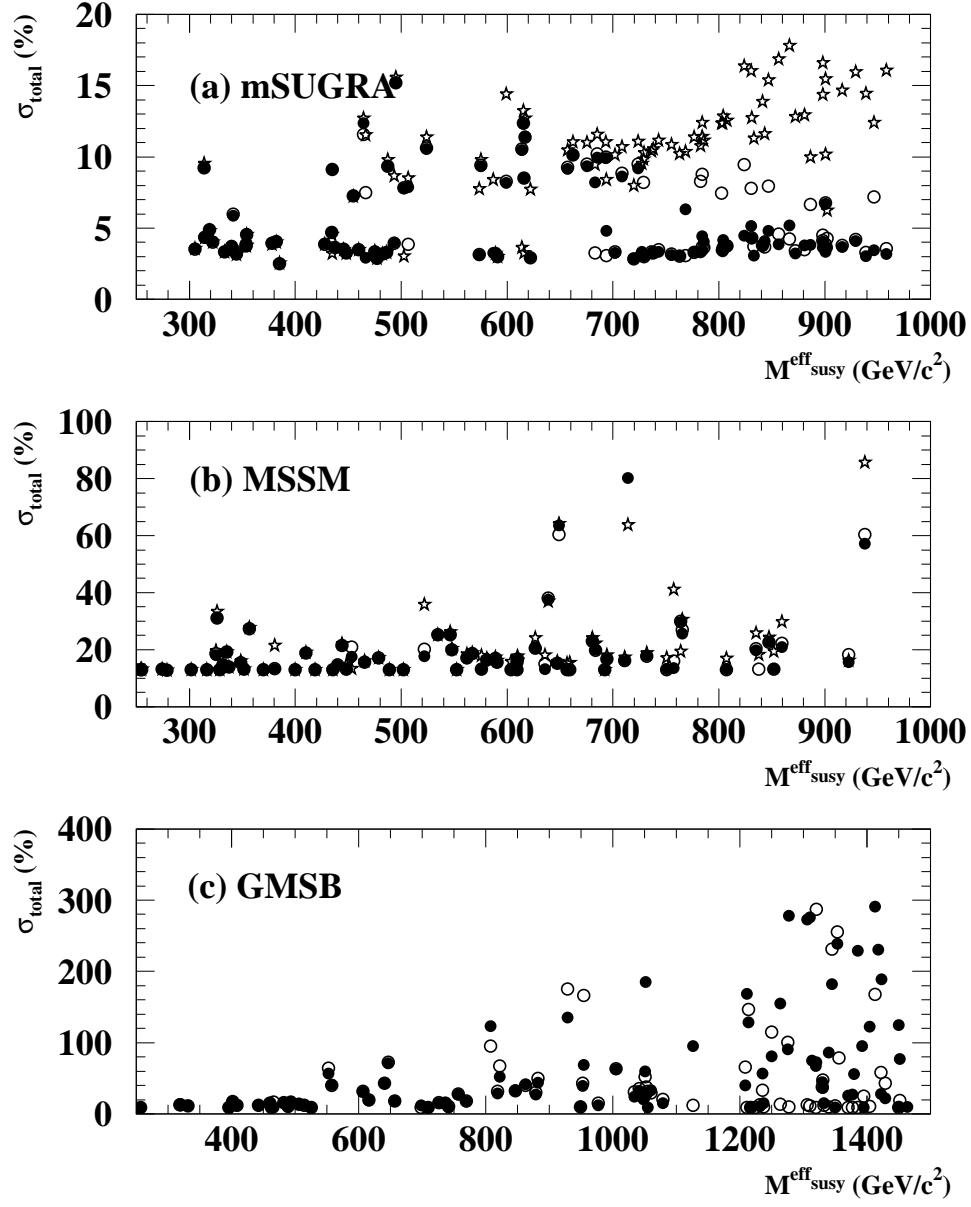


Figure 3:

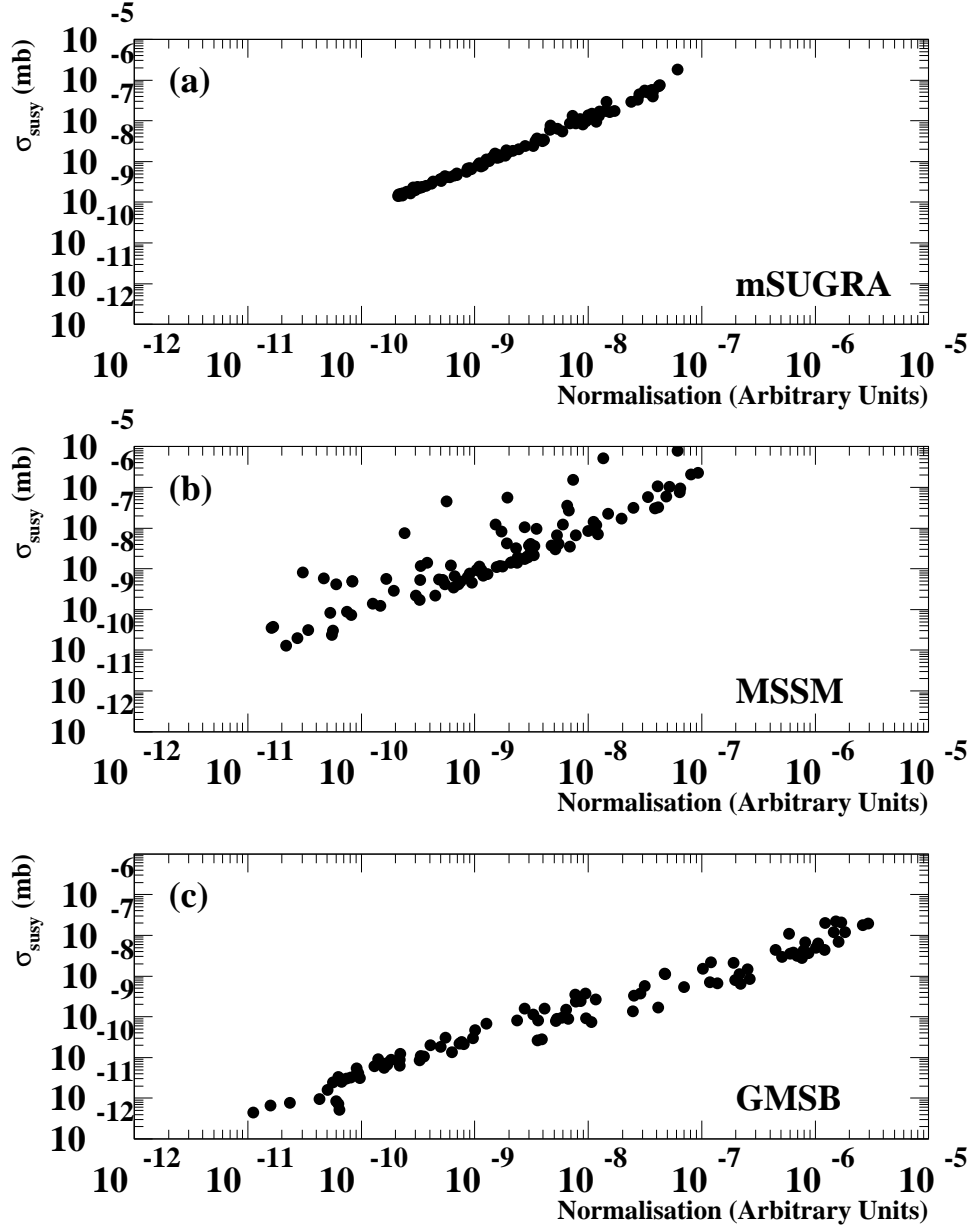


Figure 4:

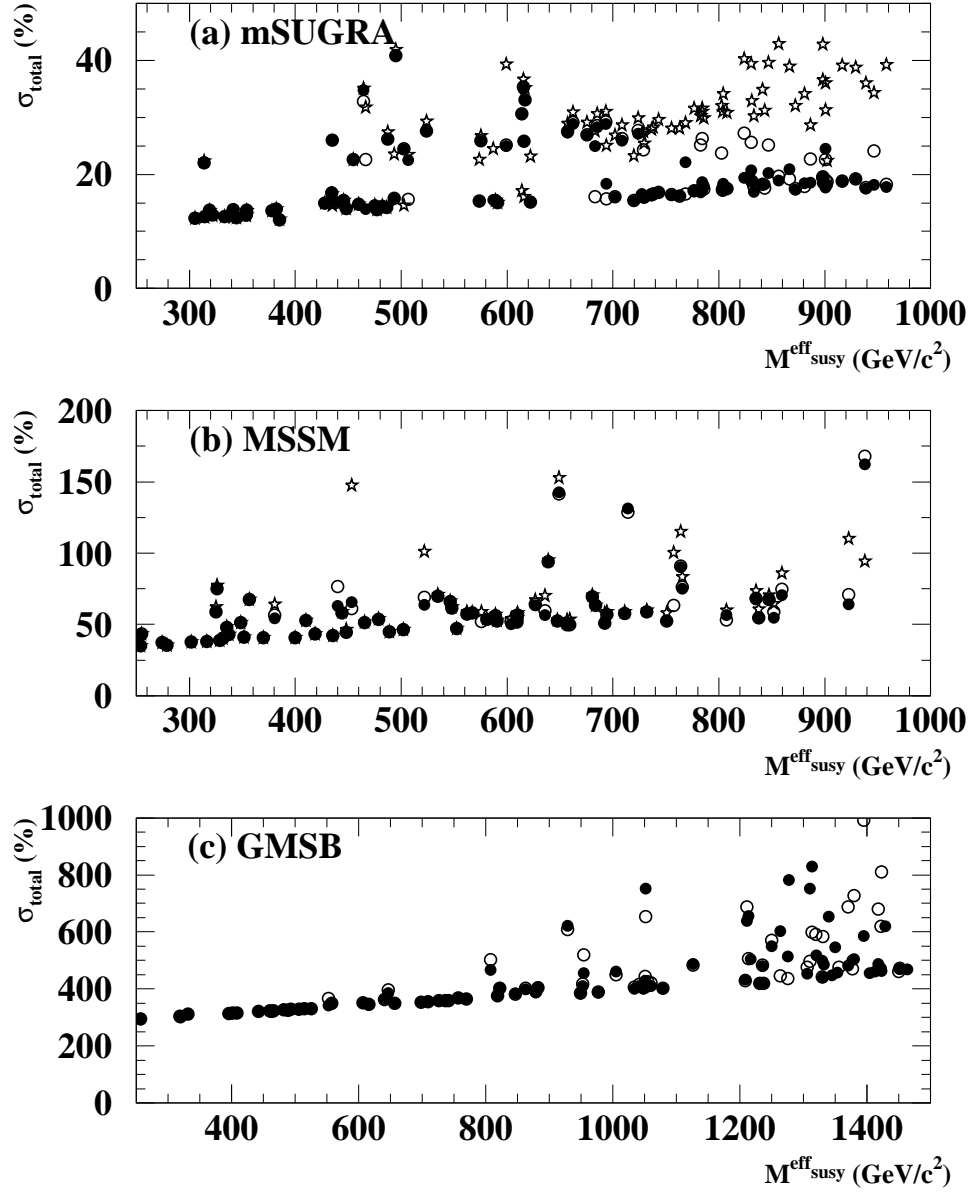


Figure 5: